Scientia Iranica A (2015) 22(4), 1363–1372

SCIENTIA IRANICA

Sharif University of Technology
Scientia Iranica
Transactions A: Civil Engineering
www.scientiairanica.com

Analytical model for predicting the shear strength of FRP-retrofitted exterior reinforced concrete beam-column joints

H. Hejabi and M.Z. Kabir*

Department of Civil and Environmental Engineering, Amirkabir University of Technology, Hafez Ave., Tehran, Iran.

Received 23 September 2012; received in revised form 28 June 2014; accepted 5 January 2015

KEYWORDS
Analytical model;
Reinforced concrete;
FRP;
Retrofit;
Beam-column joint;
Shear stress.

Abstract. In this study, a nonlinear procedure for analysis of a membrane element of a FRP strengthened concrete beam-column joint is proposed, based on a softened truss model. The procedure employs three equations for equilibrium, three for compatibility, and six for the constitutive laws of materials. The model is capable of analysing the nonlinear behaviour of RC beam-column joints under cyclic loading, and has three major attributes: nonlinear association of stress and strain in the presence of FRP, contribution of concrete damage by means of a softening coefficient, and consideration of the bond effect between steel, FRP and concrete. The proposed model is applied to some previously tested and strengthened beam-column joints, and shows good predictions of their shear strength. The effect of various parameters on the response of a reinforced concrete beam-column joint, such as a column axial load, amount of FRP reinforcement, and FRP properties, has been studied in a parametric manner. It is observed that even a low quantity of FRP can enhance the shear capacity of the joint significantly. Also, it is observed that the axial load increases the confinement of the joint care, which, in turn, increases the shear capacity of the joint.

1. Introduction

The importance of beam-column joints in the earthquake resistance capacity of reinforced concrete frames was first recognized from earthquakes in the 1960s. Since that time, researchers have made efforts to develop and improve seismic design provisions for RC joints. The prime reason behind joint failure was identified as the inadequate shear strength of the joint. Inadequate joint shear strength is generally due to insufficient and inadequately detailed reinforcement in the joint region. Further, due to insufficient reinforcement, particularly transverse reinforcement in the joint, joint brittleness increases, which, in turn, significantly reduces the overall ductility of the structure. The rehabilitation of beam-column joints represents a feasible approach to mitigate hazards in existing structures and to provide safety for their occupants. In the last few decades, the strengthening of existing seismically deficient joints has received considerable attention. Several rehabilitation schemes for strengthening joints were proposed one of which is FRP strengthening. The use of FRP composites for strengthening is a relatively modern concept and, generally, most effective, due to advantages like fast and easy application, high strength/weight ratio, and corrosion resistance.

Analytical modelling of FRP-strengthened joints has been limited. Gergely et al. [1,2] computed FRP contributions to the shear capacity of RC joints by

*. *Corresponding author. Tel.: +98 21 64543016*
E-mail addresses: h.hejabi@aut.ac.ir (H. Hejabi); mzkabir@aut.ac.ir (M.Z. Kabir)

an analogy to steel stirrups. Ghobarrah and Said [3] proposed a design methodology for the fibre jacketing of existing beam-column joints in RC moment resisting frames. Ghobarrahand El-Amoury [4] proposed a simple design methodology for upgrading reinforced beam-column joints using GFRP sheets. Antonopoulos and Triantafillou [5] proposed a method that uses stress equilibrium and strain compatibility to yield the shear strength of the RC joint with externally bonded FRP. Almusallam and Al-Salloum [6] extended this model to predict some governing parameters, such as diagonal tensile stress, variation of shear stress in the joint at different stages of loading, and strains in transverse and longitudinal steel bars.

FRP jacketing of the joint area restricts the dilation tendency of the confined core by controlling the extent of internal damage. Damage or loss of concrete stiffness is influenced by its micro-structural properties, which is best represented by the amount of damage or expansion of the concrete core area resisting the axial loads. Internal damage is best represented using the radial strain to account for the lateral dilation of confined concrete and the corresponding loss of stiffness of FRP-confined concrete sections.

The initial response of FRP-confined concrete follows a similar behaviour to unconfined concrete, since the radial expansion of the concrete core is insignificant. By increasing the strain, micro-cracking of the concrete core starts to accumulate and the response of confined concrete deviates from elastic theory by confinement effects in a direction perpendicular to the fibre direction.

In this study, the softened truss model proposed by Hsu [7] is expanded to take into account the FRP confinement and steel and FRP bond effects, in analysing the FRP retrofitted RC joints. The proposed model has three major attributes. The first is the nonlinear association of stress and strain in the presence of FRP. The second is the contribution of concrete damage by means of softening the coefficient, which represents the steel and FRP existence of the damage parameter, and the third is consideration of the bond effect between steel and FRP and concrete. The proposed model is applied to some previously tested, strengthened beam-column joints and shows good predictions of the shear strength of these joints.

2. Mechanics of RC joints strengthened with FRP strips

2.1. Basic assumptions

A typical beam-column joint is illustrated in Figure 1. The joint is idealized as a 3D element with dimension d (width of column), b (width of beam), and h (height of beam), as shown in Figure 2. Shear stresses

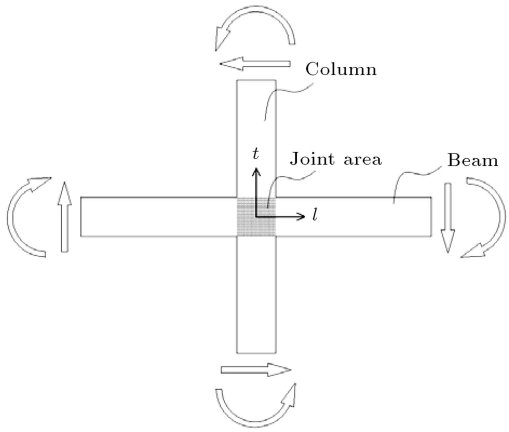

Figure 1. Moment and shear acting at joint.

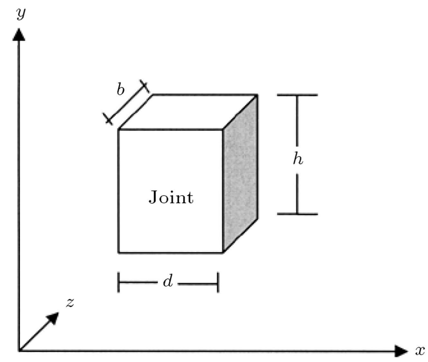

Figure 2. Dimensions of joint.

are assumed to be a bidirectional action, which is developed by the bond between reinforcement and concrete. For simplicity, it is assumed that the shear stress, τ, is uniformly distributed over the boundaries of the joint.

In this model, it is assumed that the considered element has an orthogonal grid of reinforcement in l and t directions, parallel to the element boundaries and uniformly distributed in each reinforcing direction. Thus, the cracked concrete behaves as an orthotropic material, whose material axes are aligned in the direction of principal stress (Figure 3). Also, it is assumed that the direction of principal strain is assumed to coincide with the direction of principal stress.

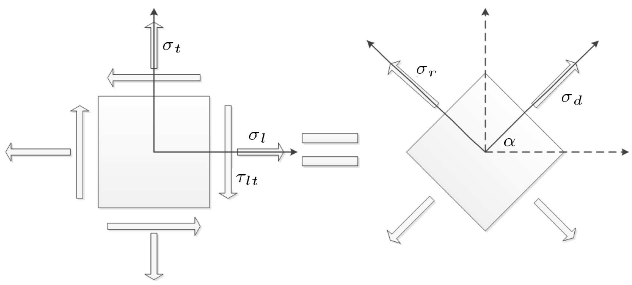

Figure 3. The coordinate system d−r in the post-cracking stage in reinforced concrete membrane elements.

2.2. Problem formulation

The states of average stress and average strain in concrete are expressed by the second order tensors:

$$\varepsilon=\begin{bmatrix}\varepsilon_l & 0.5\gamma_{lt}\\ 0.5\gamma_{lt} & \varepsilon_t\end{bmatrix}, \tag{1}$$

$$\sigma=\begin{bmatrix}\sigma_l & \tau_{lt}\\ \tau_{lt} & \sigma_t\end{bmatrix}, \tag{2}$$

where σ_l and σ_t are the average concrete normal stresses in the l and t directions, respectively; τ_{lt} is the shear stress; ε_l and ε_t are the average normal strains in the l and t directions, respectively; and γ_{lt} is the average shear strain in the $l-t$ coordinate. The convention used here is tension positive.

$$\sigma_l+\sigma_t=\sigma_d+\sigma_r, \tag{3}$$

$$\sigma_l\sigma_t-\tau_{lt}^2=\sigma_d\sigma_r, \tag{4}$$

$$\varepsilon_l+\varepsilon_t=\varepsilon_d+\varepsilon_r, \tag{5}$$

$$\varepsilon_l\varepsilon_t-0.25\gamma_{lt}^2=\varepsilon_d\varepsilon_r. \tag{6}$$

The proposed model employs 12 equations to determine the features of the behaviour of membrane elements subjected to 2-dimensional loading. These equations are 3 for equilibrium, 3 for compatibility and 6 for the constitutive laws of materials, which are based on biaxial, nonlinear and accurate constitutive equations.

2.3. Equilibrium equations

The equilibrium equations are as follows:

$$\sigma_l=\sigma_d\cos^2\alpha+\sigma_r\sin^2\alpha+(\rho_c+\beta_l\rho_{cs})f_l+\rho_{fl}f_{fl}, \tag{7}$$

$$\sigma_t=\sigma_d\sin^2\alpha+\sigma_r\cos^2\alpha+(\rho_b+\beta_t\rho_{bs})f_t+\rho_{ft}f_{ft}, \tag{8}$$

$$\tau_{lt}=(-\sigma_d+\sigma_r)\sin\alpha\cos\alpha, \tag{9}$$

where ρ_{cs} is the column reinforcement ratio inside the joint core; ρ_c is the total main column reinforcement ratio; ρ_{bs} is the stirrup reinforcement ratio; ρ_b is the total main beam reinforcement ratio; ρ_{fl} is the FRP reinforcement ratio in the longitudinal direction; ρ_{ft} is the FRP reinforcement ratio in the transverse direction; β_l is the factor that relates the magnitude of stresses in the column reinforcement outside the core to the average stresses of the reinforcement inside the core at the beam centerline; β_t is the factor that relates the magnitude of stresses in the main beam reinforcement to the average stirrup stresses at the column centerline; f_l and f_t are the average stresses in the longitudinal and transverse steel bars, respectively; f_{fl} and f_{ft} are the average normal stress in the FRP in the longitudinal and transverse directions; and α is the angle of inclination between the longitudinal axis and d axis.

2.4. Compatibility

The two-dimensional compatibility condition expresses the relationship among the average strains in different coordinate systems. In order to find out the longitudinal and transverse steel and FRP strains at failure, the strain compatibility condition should be investigated as follows:

$$\varepsilon_l=\varepsilon_d\cos^2\alpha+\varepsilon_r\sin^2\alpha, \tag{10}$$

$$\varepsilon_t=\varepsilon_d\sin^2\alpha+\varepsilon_r\cos^2\alpha, \tag{11}$$

$$\frac{\gamma_{lt}}{2}=(-\varepsilon_d+\varepsilon_r)\sin\alpha\cos\alpha, \tag{12}$$

where ε_r and ε_d are the average and normal strains in the r and d directions, respectively. The angle of inclination between the longitudinal axis and the d axis is computed as follows:

$$\tan^{-1}\alpha=\frac{\varepsilon_l-\varepsilon_d}{\varepsilon_t-\varepsilon_d}. \tag{13}$$

Because of the necessity to express the strain in the $l-t$ coordinate in terms of strain and stress in the $r-d$ coordinate, the following equations are used (based on Eqs. (3), (5), (7), (8), (10) and (11)):

$$\varepsilon_l=\varepsilon_r+\frac{\varepsilon_r-\varepsilon_d}{\sigma_r-\sigma_d}\left(\sigma_l-\sigma_r-\rho_l f_l-\rho_{fl}f_{fl}\right), \tag{14}$$

$$\varepsilon_t=\varepsilon_r+\frac{\varepsilon_r-\varepsilon_d}{\sigma_r-\sigma_d}\left(\sigma_t-\sigma_r-\rho_t f_t-\rho_{ft}f_{ft}\right). \tag{15}$$

2.5. Constitutive laws

The relationship between stress and strain along the principal compressive direction can be described by the unified constitutive law for FRP confined concrete proposed by Wei and Wu [8] in the following form:

$$\begin{cases}\sigma_d=E_c\varepsilon_c+\frac{f_0-E_c\varepsilon_0}{\varepsilon_0^2}\varepsilon_c^2 & 0\le\varepsilon_c\le\varepsilon_0\\ \sigma_d=f_0+E_2(\varepsilon_c-\varepsilon_0) & \varepsilon_0\le\varepsilon_c\le\varepsilon_{cu}\end{cases} \tag{16}$$

$$\varepsilon_0=\frac{(f_0+f_{cu}+E_c\varepsilon_{cu})-\sqrt{(f_0+f_{cu}+E_c\varepsilon_{cu})^2-8f_0E_c\varepsilon_{cu}}}{2E_c}, \tag{17}$$

$$E_2=\frac{f_{cu}-f_0}{\varepsilon_{cu}-\varepsilon_0}, \tag{18}$$

where E_c is the secant modulus of concrete; f_0 and ε_0 are the transitional stress and strain, respectively; f_{cu} and ε_{cu} are concrete ultimate stress and strain, respectively; and E_2 is the slope of the second portion in the confined concrete stress-strain curve. This model is based on the regression analysis of available experimental data for three parameters, including ultimate stress, f_{lu}, ultimate strain, ε_{Cu}, and transitional stress, f_0. Due to the paper length limits, details on calculation of current parameters are not presented here. This information can be found in Wei and Wu [8].

Observations on cracked reinforced concrete in compression indicate lower strength and stiffness than unusually compressed concrete, which is called the compression softening phenomenon [9]. It is believed that the shear strength of the beam-column joint should also be governed by the softening effect of concrete. The softening coefficient is computed as follows [9]:

$$\zeta = \frac{1 + \rho_s \times f_y/f_0}{0.85 - 0.34 \times (-\varepsilon_d/\varepsilon_0)}. \tag{19}$$

The shear resistance of reinforced concrete membrane elements also influences the tensile stress-strain relationship of concrete. A typical tensile stress-strain curve of concrete consists of two parts: 1) The ascending linear portion up to the cracking tensile strain and, 2) The descending nonlinear portion. The stress-strain relationship can be expressed by:

$$\begin{cases} \sigma_c = E_c\varepsilon_c & \varepsilon_r \leq \varepsilon_{cr} \\ \sigma_c = f_{cr}\left(\frac{\varepsilon_{cr}}{\varepsilon_c}\right)^{0.4} & \varepsilon_r \geq \varepsilon_{cr} \end{cases} \tag{20}$$

where:

$$E_c = \frac{2f'_c}{\varepsilon_0}; \quad \varepsilon_{cr} = 0.00008; \quad f_{cr} = 0.31\sqrt{f'_c}. \tag{21}$$

Reinforcement steel is usually modelled as a linear elastic, linear strain hardening material with a yield stress, f_y.

$$\begin{cases} f_s = E_s\varepsilon_s & \varepsilon_s \leq \varepsilon_y \\ f_s = f_{sy} & \varepsilon_s \leq \varepsilon_y \end{cases} \tag{22}$$

However, when reinforcing bars are surrounded by concrete, the average behavior of the stress-strain relation is quite different. The most influential difference between bare reinforcement steel and concrete surrounded steel is the lowering of the yield stress below f_y in the latter, both in tension and compression. Yielding of an RC member occurs when the steel stress at a cracked section reaches the yield stress of the bare bar. However, the average steel stress at a cracked element still maintains an elastic stress that is less than the yield strength, because the concrete matrix located between the cracks is still partially capable of resisting tensile forces, owing to the bond between the concrete and the reinforcement. Determination of element stiffness on the basis of the yielding of steel at a cracked section, where a local stress concentration appears in the steel, may result in overestimating the structural response in the post-yielding range. Since this phenomenon is accelerated with increased deformation, an analysis of RC members subjected to cyclic loading accompanying relatively large deformations requires the use of average stress-strain relations. Accordingly, the average stress-strain relation of steel needs to be defined for tracing the cracking behavior of RC beams and/or columns up to the ultimate limit state. This can be accomplished using a smeared crack model in which the local displacement discontinuities at cracks are distributed over some tributary area within the finite element, and where the behavior of cracked concrete is represented by the average stress-strain relations. Considering these factors, the following linear average stress-strain relation, introduced by Belarbi and Hsu [10] from experimental data, is used:

$$\begin{cases} f_s = E_s\varepsilon_s & \varepsilon_s \leq \varepsilon_n \\ f_s = f_n + (0.02 + 0.25B)E_s(\varepsilon_s - \varepsilon_n) & \varepsilon_s \geq \varepsilon_n \end{cases} \tag{23}$$

$$B = \frac{1}{\rho}\left(\frac{f_{cr}}{f_y}\right)^{1.5} \tag{24}$$

$$\begin{cases} \varepsilon_n = \varepsilon_y(0.93 - 2B) \\ f_n = E_s\varepsilon_n \end{cases} \tag{25}$$

where f_s and ε_s represent the average strain and stress, respectively, and f_y and ε_y are the yield stress and the corresponding yield strain of a bare steel bar, respectively. f_s becomes f_l and f_t when applied to longitudinal and transverse steel.

The FRP is assumed to behave elastically until failure or debonding. It will fail by tensile fracture when the tensile stress reaches the tensile strength.

$$f_f = E_f\varepsilon_f, \tag{26}$$

f_f and ε_f represent the average FRP strain and stress, respectively, and becomes f_{fl}, f_{ft}, ε_{fl} and ε_{ft} when applied to longitudinal and transverse FRP sheets. Also, depending on how it is treated, according to the model by Islam and Wu, FRP debonding load is calculated as follows:

$$\begin{cases} f_{f,deb} = 0.565 b_f f_c'^{0.1}(E_f t_f) & l_b \geq L_{be} \\ f_{f,deb} = 0.565 b_f f_c'^{0.1}(E_f t_f)\left(\frac{l_b}{L_{be}}\right) & l_b \leq L_{be} \end{cases} \tag{27}$$

$$L_{fe} = 0.395\frac{(E_f t_f)^{0.54}}{f_c'^{0.09}}, \tag{28}$$

where b_f is FRP layer width. FRP systems that are not anchored have been observed to delaminate from the concrete before the loss of aggregate interlock of the section. For this reason, bond stresses should be analyzed to determine the effective strain level that can be achieved. The effective strain is calculated using a bond-reduction coefficient, k_v, applicable to shear:

$$\varepsilon_{fe} = k_v \varepsilon_{fu} \leq 0.004. \tag{29}$$

The bond-reduction coefficient is a function of the concrete strength, the type of wrapping scheme used, and the stiffness of the laminate. In this research, the bond-reduction coefficient is computed from the equations of ACI440-02 [11] proposed by Khalifa et al. [12]:

$$k_v = \frac{k_1 k_2 L_e}{11900\varepsilon_{fu}} \leq 0.75. \tag{30}$$

This equation relies on the active bond length, L_e, which is the length over which the majority of the bond stress is maintained, and two modification factors, k_1 and k_2, that account for the concrete strength and the type of FRP scheme used, respectively. Expressions for these parameters are given as follows:

$$L_e = \frac{23300}{(t_f E_f)^{0.58}}, \tag{31}$$

$$k_1 = \left(\frac{f'_c}{27}\right)^{2/3}, \tag{32}$$

$$k_2 = \frac{h - 2L_e}{h}. \tag{33}$$

Furthermore, it is noted that if, at the moment of strengthening, the joint is already loaded, a set of initial normal strains, e_{0t} and e_{0l}, in the transverse (beam) and longitudinal (column) direction, respectively, initial shear strain, γ_0, can be defined and enters the equilibrium equations. These parts act as constant parts in solving equations and have no effect on solution procedure.

3. Solution procedure

The analytical formulation given above was implemented in a computer program specifically developed for the analysis of RC joints strengthened with FRP strips. The user inputs a series of material and geometric characteristics, and the program traces the state of stress and strain in the joint until failure. Input to the program consists of:

1. The geometric variables, ρ_c, ρ_b, ρ_{cs}, ρ_{bs}, ρ_{fl}, ρ_{ft}; b, h, w;
2. The bond condition variables, β_t and β_l (Eqs. (7) and (8));
3. The material properties, f_c, f_{cr}, and e_0 for concrete; E_s, f_{yl}, f_{ys}, and f_{yt} for steel, and E_f, f_{fu}, and $f_{f,deb}$ for FRP;
4. The axial forces, N_l and N_t; and
5. The initial strains, e_{0l} and e_{0t}, in the joint (at the moment of strengthening).

The solution procedure is described in the following steps (Figure 4):

1. Assume ε_d;

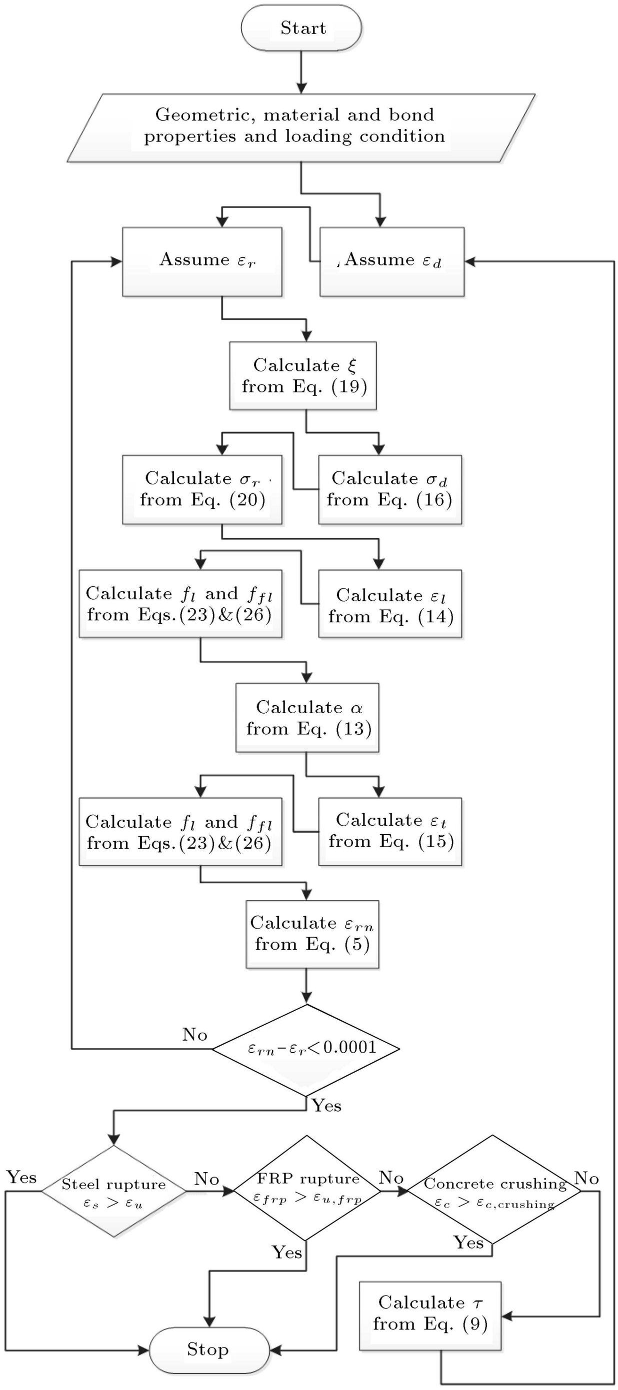

Figure 4. Maximum shear stress calculation flowchart.

Table 1. Specimen description.

Specimen	Beam		Column		Anchorage	f_c MPa	Reinforcement				FRP			
	H (mm)	b (mm)	w (mm)	b (mm)			ρ_{sl}	ρ_{st}	f_{yl} (MPa)	f_{ys} (MPa)	ρ_{fl}	ρ_{ft}	E_y (MPa)	ε_{fu}
Al(IC1)	160	350	300	160	No	30	1.6%	1.6%	420	420	-	-	-	-
Al(IC2)	160	350	300	160	No	25	1.6%	1.6%	420	420	-	-	-	-
Al(IS1)	160	350	300	160	No	30	1.6%	1.6%	420	420	1.25%	0	61.5	
Al(IS2)	160	350	300	160	Yes	25	1.6%	1.6%	420	420	1.25%	0	61.5	
ANT(C)	300	200	200	200	No	21.6*	1.54	1.54	585	585	-	-	-	-
ANT(F11)	300	200	200	200	No	22.8*	1.54	1.54	585	585	0.13	0.13	230	0.016
ANT(F21)	300	200	200	200	No	27*	1.54	1.54	585	585	0.26	0.13	230	0.016
ANT(F22)	300	200	200	200	No	27.2*	1.54	1.54	585	585	0.26	0.26	230	0.016
ANT(F22W)	300	200	200	200	Yes	29.2*	1.54	1.54	585	585	0.26	0.26	230	0.016

*Cube specimen strength.

2. Assume ε_r;
3. Calculate softening coefficient from Eq. (19);
4. Calculate σ_d from Eq. (16);
5. Calculate σ_r from Eq. (20);
6. Calculate ε_l from Eq. (14) by consideration of bond effects from Eqs. (25) and (32);
7. Calculate f_l from Eq. (25);
8. Calculate f_{fl} from Eq. (28);
9. Calculate α from Eq. (13);
10. Calculate ε_t from Eq. (15) by consideration of bond effects from Eqs. (25) and (32);
11. Calculate f_t from Eq. (25);
12. Calculate f_{fl} from Eq. (28);
13. Calculate ε_r from Eq. (5);
14. If the difference between the calculated ε_r and the assumed value of ε_r is small, then proceed. Otherwise, go to the beginning of the loop and increase ε_r;
15. Control steel rupture; if ultimate strain is reached, go to step 18, otherwise, proceed;
16. Control FRP rupture; if ultimate strain is reached, go to step 18, otherwise, proceed;
17. Control concrete crashing; if ultimate strain is reached, go to step 18, otherwise, go to step 1;
18. Calculate shear stress for assumed ε_d from Eq. (9).

4. Verification of the analytical model

In order to have sufficient confidence in the above-presented algorithm, it was necessary to compare the shear capacity from the proposed procedure with some experimental test results available in the literature. However, experimental data on FRP-strengthened beam-column joints have been relatively limited. For this purpose, the experimental work of Almusallam and Al-Salloum [13] and Antonopoulos and Triantafillou [14] on exterior joints was selected for validation. The key data for analysis of these specimens are given in Table 1, and comparison between experimental results and the results of analysis with the proposed procedure are given in Table 2. A detailed description of the specimens; geometries and material properties of concrete, steel and FRP; test set up; and instrumentation details can be seen in Almusallam and Al-Salloum [13] and Antonopoulos and Triantafillou [14]. Based on this comparison, it is concluded that the agreement between the proposed algorithm and test results is good, and the proposed procedure may be used to design an externally bonded retrofit for beam-column joints.

Table 2. Verification of the analytical model: Analysis results.

Specimen	ν Experimental (MPa)	ν Analytical (MPa)	Anal./ Exp.*
Al(IC1)	6.36	6.26	0.98
Al(IC2)	4.95	5.18	1.05
Al(IS1)	7.39	7.88	1.06
Al(IS2)	7.17	6.85	0.96
ANT(C)	3.2	3.18	0.99
ANT(F11)	4.64	4.60	0.99
ANT(F21)	5.47	5.24	0.96
ANT(F22)	5.37	5.40	1.01
ANT(F22W)	6.15	5.87	0.95

*Analytically calculated shear strength divided by experimentally one.

5. Parametric study

In this section, the effect of the quantity of FRP reinforcement on a parametric basis, using the proposed procedure, is studied. For this reason, a joint with the following characteristics were studied: The joint is

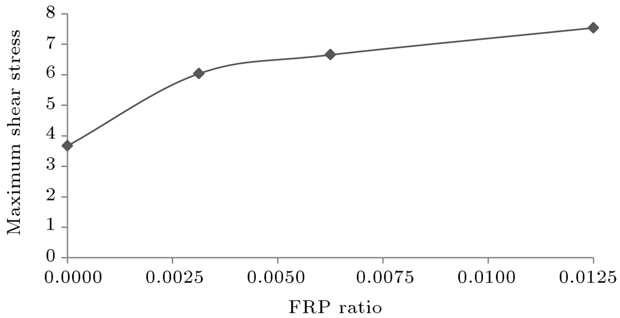

Figure 5. Effect of FRP reinforcement on shear strength of the joint.

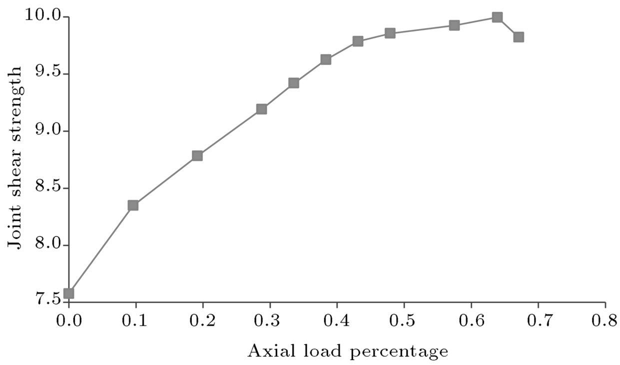

Figure 6. Effect of axial load on shear strength of the joint.

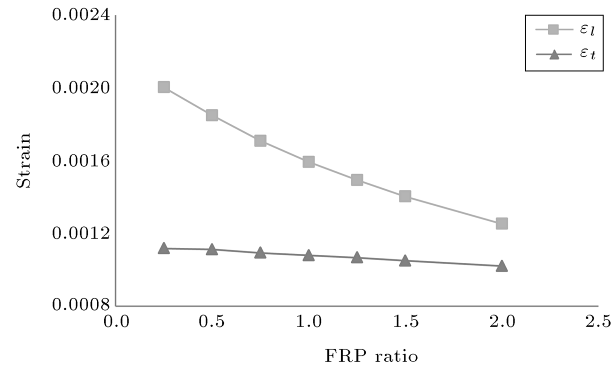

Figure 7. Effect of FRP reinforcement on beam and column reinforcement strains.

assumed to be reinforced equally in the column and the beam ($\rho_c = \rho_b = 0.015$). Each FRP layer consists of unidirectional carbon fibers in an epoxy matrix, and has an elastic modulus equal to 180 GPa and ultimate strain equal to 1.2%. Joint dimensions are 500 (column height) $\times$ 500 (beam height) $\times$ 250 (column and beam width). The elastic modulus and yield stress of column and beam reinforcements are 200 GPa and 420 MPa, respectively. The compressive strength of concrete is assumed equal to 25 MPa, and its ultimate strain is assumed to be 0.0021.

First, the variation of joint shear strength with the amount of FRP, keeping all other parameters the same, is studied. The result of the analysis is shown in Figure 5. As shown, a small increase in the amount of FRP considerably increases the shear strength of the joint. This can be attributed to the confinement of the joint core. As the quantity of FRP increases, confinement increases, which, in turn, increases the shear strength of the joint. Also, the effectiveness of FRP improves as more fibers are placed in the beam direction (perpendicular to the column direction, which includes axial load). As shown in Figure 5, the maximum shear stress diagram has two distinctive slopes. These denote that the rate of increase in the maximum shear stress of the joint slows down after a specific amount of FRP reinforcement, and an increase in the amount of FRP beyond this limit is not particularly effective.

The variation of maximum shear stress of the joint with column axial load is shown in Figure 6. It is indicated in the figure that maximum joint shear stress increases by increasing axial load. This is due to the fact that with an increase in axial load, confinement of the joint core increases, which, in turn, increases the shear capacity of the joint.

Also, variations of the joint transverse, longitudinal and shear strain of a FRP retrofitted joint were studied. As expected, the magnitude of maximum strain decreases with the increase of FRP quantity. This can be attributed to redistribution of load due to the additional reinforcement provided by the FRP. In Figure 7, variations of the beam (ε_l) and column (ε_t) maximum strains in a FRP retrofitted RC joint with fibers in the beam direction (to ensure the maximum confinement effectiveness of the retrofit scheme) are presented. As shown in this figure, both strains are reduced, but, the rate of degradation in the beam direction is much more than the equivalent rate in the column direction.

Finally, the effect of fiber direction was studied parametrically. For this reason, a joint retrofitted with constant amounts of FRP, but with different portions in the beam and column directions, is described as follows (V_t is FRP volume portion in the column direction, and V_l is FRP volume portion in the beam direction):

1. $V_t : V_l = 1$, which represent 100% fibers in the column direction;
2. $V_t : V_l = 0.75$, which represent 75% fibers in the column direction and 25% in the beam direction;
3. $V_t : V_l = 0.5$, which represent 50% fibers in both column and beam directions;
4. $V_t : V_l = 0.25$, which represent 25% fibers in the column direction and 75% in the beam direction;
5. $V_t/V_l = 0$, which represent 100% fibers in the beam direction.

In Figures 8-10, variations of joint maximum

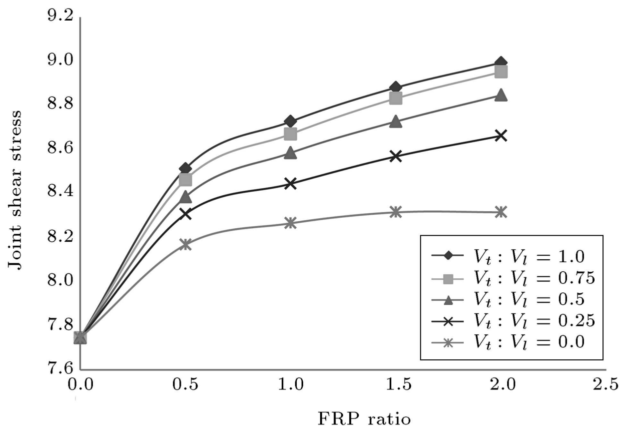

Figure 8. Effect of FRP reinforcement configuration on maximum joint shear stress.

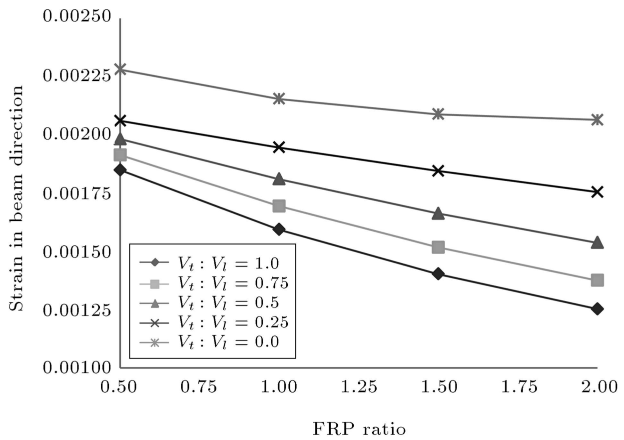

Figure 9. Effect of FRP reinforcement configuration on maximum beam direction strain.

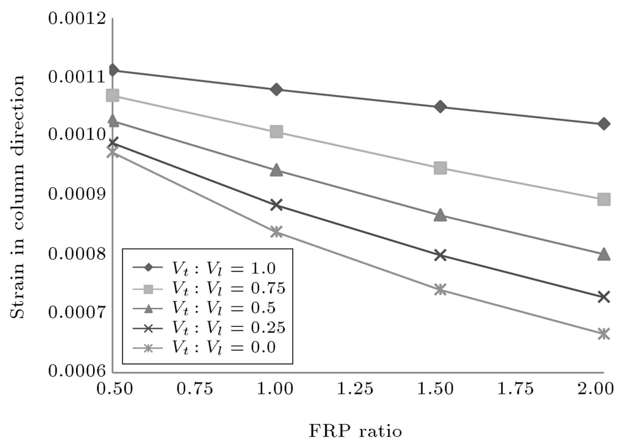

Figure 10. Effect of FRP reinforcement configuration on maximum column direction strain.

shear stress in the concrete core, beam strains and column strains are represented. As shown in these figures, confinement effects of the beam direction fibres (because of the presence of axial load in the column direction) made retrofit in the beam direction efficient for the shear strengthening of an edge RC joint.

6. Conclusions

An algorithm for determining the shear strength of FRP retrofitted exterior beam-column joints under seismic action is proposed. The algorithm uses the softened truss concept, proposed by Hsu [7], to analyze a reinforced concrete beam-column joint retrofitted with FRP. For more accuracy in analysis, the nonlinear association of stress and strain in the presence of FRP, the contribution of concrete damage and consideration of the bond effect between steel and FRP and concrete were considered. The model can provide valuable insight into the seismic behavior of retrofitted exterior beam-column joints, and is able to evaluate the seismicity of existing joints.

Parametric analyses using the proposed model indicated that even low quantities of FRP material may provide significant enhancement of the shear capacity. The effectiveness of external reinforcement depends on the configuration of layers on joint regions, the beam and the column, amount of column axial load, and the relative quantities of steel and FRP reinforcement in the beam and column directions that cross the joint panel. It was observed that with an increase in the quantity of horizontally directed FRP layers in the joint region, with the existence of axial load in columns, confinement increases, which causes an increase in the shear strength of the joint. Also, the maximum shear stress diagram shows two distinctive slopes, which indicates that the rate of increase in the maximum shear stress of the joint slows down after a specific amount of FRP reinforcement, and that an increase in the amount of FRP beyond this limit is not particularly effective. The formulation could be extended for layered composites with different fiber orientations with few changes in formulation. It is also extendible to 3D analysis of retrofitted joints by writing equations in tensor form and introducing damage factors, which will be discussed in another article by the authors.

Nomenclature

γ_{lt}	Average shear strain in $l-t$ coordinate (mm/mm)
τ_{lt}	Average stress strain in $l-t$ coordinate (MPa)
k_v	Bond-dependent coefficient for shear
ε_0	Strain at the maximum compressive stress of non-softened concrete (mm/mm)
ε_c	Strain level in the concrete (mm/mm)
ε_{cr}	Concrete cracking tensile strain (mm/mm)

ε_d	Average principal (compressive) strain in concrete in d direction (mm/mm)
ε_{fe}	Effective strain level in FRP reinforcement; strain level attained at section failure (mm/mm)
ε_{fu}	Mean rupture stain of FRP reinforcement (mm/mm)
ε_{cu}	Ultimate concrete strain (mm/mm)
ε_l	Average strain in longitudinal direction (mm/mm)
ε_r	Average principal (tensile) strain in concrete in r direction (mm/mm)
ε_t	Average strain in transverse direction (mm/mm)
σ_d	Average principal (compressive) stress in concrete in d direction (MPa)
σ_l	Average stress in longitudinal direction (MPa)
σ_r	Average principal (tensile) stress in concrete in r direction (MPa)
σ_t	Average stress in transverse direction (MPa)
b	Beam width
b_f	FRP width
d	Column width
E_c	Secant modulus of concrete (MPa)
E_f	FRP strips elastic modulus in principal fiber direction (MPa)
E_s	Steel elastic modulus (MPa)
E_2	Slope of second portion in confined concrete stress-strain curve (MPa)
f'_c	Unconfined strength of concrete in compression
f_{cr}	Mean tensile strength of concrete
f_y	Reinforcement yield stress
h	Beam height
l_b	FRP bond length
ρ_{cs}	Column reinforcement ratio inside the joint core
ρ_c	Total main column reinforcement ratio
ρ_{bs}	Stirrup reinforcement ratio
ρ_b	Total main beam reinforcement ratio
ρ_{fl}	FRP reinforcement ratio in the longitudinal direction
ρ_{ft}	FRP reinforcement ratio in the transverse direction
β_l	Factor that relates the magnitude of stresses in the column reinforcement outside the core to the average stresses of the reinforcement inside the core at the beam centerline
β_t	Factor that relates the magnitude of stresses in the main beam reinforcement to the average stirrup stresses at the column centerline
f_l	Average stress in longitudinal steel bars
f_t	Average stress in transverse steel bars
f_{fl}	Average normal stress in the FRP in the longitudinal direction
f_{ft}	Average normal stress in the FRP in the transverse direction
α	Angle of inclination between the longitudinal axis and d axis
l_b	FRP bond length
$f_{f,deb}$	Maximum tensile stress in FRP when debonding occurs
f_{fu}	Ultimate tensile strength in primary fiber direction

References

1. Gergely, J., Pantelides, C.P., Nuismer, R.J. and Reaveley, L.D. "Bridge pier retrofit using fiber-reinforced plastic composites", *Journal of Composite Construction*, **2**(4), pp. 165-174 (1998).
2. Gergely, J., Pantelides, C.P. and Reaveley, L.D. "Shear strengthening of RCT-joints using CFRP composites", *Journal of Composite Construction*, **4**(2), pp. 56-64 (2000).
3. Ghobarrah, A. and Said, A. "Seismic rehabilitation of beam-column joints using FRP laminates", *Journal of Earthquake Engineering*, **5**(1), pp. 113-129 (2001).
4. Ghobarrah, A. and El-Amoury, T. "Seismic rehabilitation of deficient exterior concrete frame joints", *Journal of Composite Construction*, **9**(5), pp. 408-416 (2005).
5. Antonopoulos, C.P. and Triantafillou, T.C. "Analysis of FRP-strengthened RC beam-column joints", *Journal of Composites for Construction*, **6**(1), pp. 41-51 (2002).
6. Al-Salloum, Y.A. and Almusallam, T.H. "Seismic response of interior RC beam-column joints upgraded with FRP sheets: II: Analysis and parametric study", *Journal of Composites for Construction*, **11**(6), pp. 590-600 (2007).
7. Hsu, T.T.C. and Mo, Y.L., *Unified Theory of Concrete Structures*, John Wiley & Sons Ltd (2010).
8. Wei, Y.Y. and Wu, Y.F. "Unified stress-strain model of concrete for FRP confined columns", *Construction and Buildings Materials*, **26**, pp. 381-3923 (2012).

9. Vecchio, F.J. and Collins, M.P. "Compression response of cracked reinforced concrete", *Journal of Structural Engineering, ASCE*, **119**(12), pp. 3590-3610 (1993).
10. Belarbi, A. and Hsu, T.T.C. "Constitutive laws of concrete in tension and reinforcing bars stiffened by concrete", *ACI Structural Journal*, **94**(4), pp. 465-74 (1994).
11. ACI440.2R-02, *Guide for the Design and Construction of Externally Bonded FRP Systems for Strengthening Concrete Structures*, Reported by ACI Committee 440 (2002).
12. Khalifa, A., Alkhrdaji, T., Nanni, A. and Lansburg, S. "Anchorage of surface mounted FRP reinforcement", *Concrete International*, **21**, pp. 49-54 (1999).
13. Al-Salloum, Y.A. and Almusallam, T.H. "Seismic response of interior RC beam-column joints upgraded with FRP sheets. I: Experimental study", *Journal of Composites for Construction*, **11**(6), pp. 575-589 (2007).
14. Antonopoulos, C.P. and Triantafillou, T.C. "Experimental investigation of FRP-strengthened RC beam/column joints", *Journal of Composites for Construction*, **7**(1), pp. 39-49 (2003).

Biographies

Hadi Hejabi received a BS degree in Civil Engineering from Isfahan University of Technology, Iran, in 2006, and an MS degree in Structural Engineering, in 2008, from the Department of Civil Engineering at Sharif University of Technology, Tehran, Iran. He is currently finishing his PhD degree at Amir Kabir University of Technology, Tehran, Iran. His research interests include retrofitting of structures and lifelines.

Mohammad Z. Kabir is Professor and Chair of Civil and Environmental Engineering Department at Amirkabir University of Technology, Iran. He received his BS and MS degrees from Amirkabir University of Technology and his PhD degree from Waterloo University in Canada. His research interests include structural stability, structural analysis using FEM, experimental methods in structural engineering, composite structures, structural optimization, damage detection and rehabilitation of structures.